Computational Mechanics (1991) 8, 1–18

Computational Mechanics

Combined control-structural optimization

M. Milman*, M. Salama, R. E. Scheid, R. Bruno
Jet Propulsion Laboratory, California Institute of Technology, 4800 Oak Grove Drive Pasadena, CA 91109, USA

J. S. Gibson
University of California, Los Angeles, CA 90024, USA

1 Introduction

The strong interaction between structural dynamics and active control is a well-recognized challenge in the analysis of controlled flexible structures. But it is only recently that the same interaction has been exploited in the design process. The traditional design approach in which the control design comes very late in the development—typically after the structure has been designed and built—is no longer viable. Although this approach has produced satisfactory results for the attitude control of relatively rigid space structures, it will not be suitable for the ambitious space missions that require precise controlled pointing of telescopes, interferometers and the vibration suppression for science instruments mounted on large flexible structures. In such systems, designing the structure and designing its control become entwined. This dictates early consideration of the control design—well before any detailed structural design is finalized. And just as the structure is optimally designed to meet such performance metrics as minimum mass or response to external disturbances, it should be optimally designed to meet its ultimate control performance as well.

A natural way to introduce the control element into the overall design process is through an optimization procedure that combines the structural and control design criteria into a single problem formulation. Bodder and Junkins (1984), Lim and Junkins (1989), Khot et al. (1985), Morrison et al. (1988), Salama et al. (1988), Milman et al. (1989) and Hale et al. (1985) have taken this perspective. In terms of the types of design parameters and constraints considered, (Lim and Junkins 1989) is probably the most extensive in that the design variables include structure parameters, actuator locations and the elements of the feedback matrix. Static output feedback is used, and the performance objectives include total mass and robustness measures. Constraints are imposed on the eigenvalue placements, performance bounds, and structural constraints. Since not all of the constraints are commensurate, they are relaxed using a homotopy approach. Just as with Milman et al. (1989), the approach taken in the present paper is not to produce the "best" optimized point design, but to produce a family of Pareto optimal designs representing options that assist in early trade studies. The philosophy is that these are candidate designs to be passed on for further consideration, and their function is more to guide the system design rather than to represent the ultimate design.

An optimization approach that is consistent with this philosophy is to utilize multiple cost objectives that include an LQG cost criterion in conjunction with structural cost(s), and possibly other control related costs. After introducing the combined objective formulation in the setting of vector optimization, we derive the necessary conditions for Pareto optimality. No behavioral constraints are explicitly imposed in the problem formulation and a homotopy approach is used to generate a family of optimum designs. Since the primary intent of this paper is to explore this

* Part of this work was performed while the author was visiting the University of Southern California

design approach and to provide an exposition to the computational aspects of the problem using simple numerical examples, the analysis is focused on a narrow regime of problems. Thus, a number of simplifying assumptions have been made, some of which are due to limitations in the underlying analysis, while others are made to facilitate the exposition. In the appropriate sections, alternatives will be discussed for relaxing these assumptions and extending the analysis to a broader range of applicability of the design approach.

2 Combined optimization

The combined optimization approach can be best appreciated when contrasted with the traditional sequential optimization. In the sequential optimization, the structure is first optimized by selecting the design variables, $\boldsymbol{\alpha}$ (e.g. member sizes) which minimize a structural criterion $J_s(\boldsymbol{\alpha})$—often taken as the mass of the structure subject to some behavioral constraints $h(\boldsymbol{\alpha}) \geqq 0$ on deformations, stresses, open-loop frequencies, etc.

$$\min_{\boldsymbol{\alpha}} J_s(\boldsymbol{\alpha}); \quad h(\boldsymbol{\alpha}) \geqq 0, \quad \boldsymbol{\alpha} \in D \tag{2.1}$$

where D is the physical domain for $\boldsymbol{\alpha}$. Second, having completely specified the optimal structural design $\boldsymbol{\alpha}^*$, the control optimization is carried out with $\boldsymbol{\alpha}^*$ fixed. For example, LQG or H_∞ optimal control designs pose the problem:

$$\min_{\boldsymbol{C}} J_c(\boldsymbol{\alpha}^*, \boldsymbol{C}) \tag{2.2}$$

where J_c represents either of the control criterion, and $\boldsymbol{C}$ is allowed to very over the class of stabilizing compensators for the plant.

By contrast, in the combined optimization formulation, the goal is to first merge the criteria of interest (here J_s and J_c) into one using non-negative multipliers β, and δ, then optimize the combined criterion over the original design variable space $\boldsymbol{\alpha}$, $\boldsymbol{C}$:

$$\min_{\boldsymbol{\alpha}, \boldsymbol{C}} [\beta J_s(\boldsymbol{\alpha}) + \delta J_c(\boldsymbol{\alpha}, \boldsymbol{C})]. \tag{2.3}$$

The following expression compares the results of the two optimization procedures outlined above.

$$\min_{\boldsymbol{\alpha}, \boldsymbol{C}} [\beta J_s(\boldsymbol{\alpha}) + \delta J_c(\boldsymbol{\alpha}, \boldsymbol{C})] \leqq [\min_{\boldsymbol{\alpha}} \beta J_s(\boldsymbol{\alpha}) + \min_{\boldsymbol{C}} \delta J_c(\boldsymbol{\alpha}^*, \boldsymbol{C})]. \tag{2.4}$$

The right-hand side of (2.4) corresponds to performing the sequential optimization by solving (2.1) for $\boldsymbol{\alpha}^*$, followed by solving (2.2) for $\boldsymbol{C}^*$. Note that the optimal solution of the right-hand side is independent of β and δ- but not so for the combined optimization embodied by the left-hand side. In terms of the total cost, expression (2.4) states the fact that the combined optimization is never inferior to the sequential optimization. In the vector optimization setting, the relative weighting of β and δ serves as a parameter that allows the generation of an entire family of Pareto optima.

In the present paper, only two objective criteria are dealt with. But it is not difficult to generalize the approach to incorporate other criteria such as minimum open-loop frequency and certain controller robustness measures. In general these criteria are noncommensurate, and there is no unique solution that minimizes all criteria $J_1, \ldots, J_N$ simultaneously. Thus, one must look for Pareto optimal solutions as outlined below.

First one assembles the criteria $J_i: D \to R$, $i = 1, \ldots, N$ into a single criterion $J: D \to R^N$, $J(\boldsymbol{\alpha}) = (J_1(\boldsymbol{\alpha})), \ldots, (J_N(\boldsymbol{\alpha}))^T$. Then the cone $C_o = \{x \in R^N: x_i \geqq 0, i = 1, \ldots, N\}$ is defined to induce a partial ordering $\leqq$ on R^N by $\boldsymbol{x} \leqq \boldsymbol{y}$ if $\boldsymbol{y} - \boldsymbol{x} \in C_o$. Now let $\boldsymbol{\alpha} \in D$. A design vector $\boldsymbol{\alpha}^* \in D$ is said to be (strongly) Pareto optimal if $J(\boldsymbol{\alpha}) \leqq J(\boldsymbol{\alpha}^*)$ implies $J(\boldsymbol{\alpha}) = J(\boldsymbol{\alpha}^*)$. A necessary condition for Pareto optimality is contained in the following theorem due to Lin (1976).

Theorem 2.1. *If α^* is Pareto optimal for the combined criterion J, and $\mathbf{D}$ is an open set, then there exists a nonzero vector $Z \in C_o$ such that $Z^T J_*(\alpha^*) = 0$. Here J_* denotes the differential of J.*

For the two-term optimization problem in (2.3), we find that the Pareto optimal solutions to $J = (J_s, J_c)^T$ can be generated by solving for the necessary conditions for extremizing the following convex combination J_λ:

$$J_\lambda = (1-\lambda) J_s(\alpha) + \lambda J_c(\alpha, C); \quad \lambda \in [0, 1] \tag{2.5}$$

where λ replaces β, δ in (2.3). The form of Eq. (2.5) suggests a homotopy (or continuation) approach for generating a family of Pareto optima as λ is propagated from 0 to 1. Although no behavioral constraints are explicitly imposed in this paper on $J_s(\alpha)$ or $J_c(\alpha, C)$, we note that the homotopy approach has direct applicability to penalty methods for solving inequality constraint problems as well. For example, suppose that in addition to extremizing the convex combination in (2.5), one wished to include a constraint of the form $[h(\alpha) - \omega_o \geq 0]$, where $h(\alpha)$ denotes the open loop fundamental frequency of the structure and ω_o is some preselected value. To accomodate an inequality constraint of this type, define

$$g(\alpha) = \begin{cases} (h(\alpha) - \omega_o)^2, & \text{if } h(\alpha) < \omega_o; \\ 0 & \text{otherwise,} \end{cases} \tag{2.6}$$

and introduce the three-cost objective function

$$J_\lambda = (1-\lambda)\{t_s J_s + t_c J_c\} + \lambda g \tag{2.7}$$

where $t_s + t_c = 1$ with $t_s, t_c \geq 0$. Fixing t_s and t_c, and letting $\lambda \to 1$ corresponds to a penalty method for solving

$$\min_{\alpha} \{t_s J_s(\alpha) + t_c J_c(\alpha)\} \quad \text{subject to} \quad h(\alpha) \geq \omega_o. \tag{2.8}$$

Although numerical ill-conditioning could easily result as $\lambda \to 1$ if the approach above is applied directly, several refinements of this penalty method that ameliorate the conditioning problem can be formulated in this context Fletcher (1987).

3 Conditions of optimality

We begin with the n_s degree-of-freedom dynamical system

$$\mathbf{M}(\alpha)\ddot{r} + \mathbf{D}(\alpha)\dot{r} + \mathbf{K}(\alpha)r = \mathbf{G}_1 u + \mathbf{G}_2 v \tag{3.1}$$

where $\mathbf{M}$, $\mathbf{D}$, and $\mathbf{K}$ are the $n_s \times n_s$ mass, damping and stiffness, $\mathbf{G}_1$ is the constant $n_s \times n_u$ control influence matrix, and $\mathbf{G}_2$ is the constant $n_s \times n_d$ disturbance matrix. The vectors r, u, and v are respectively, physical degree-of-freedom, control forces and disturbances. Let $x = (r, \dot{r})^T$. Then the first order state equation is

$$\dot{x} = \mathbf{A}(\alpha)x + \mathbf{B}_1(\alpha)u + \mathbf{B}_2(\alpha)v + v' \tag{3.2}$$

where

$$\mathbf{A} = \begin{pmatrix} \mathbf{0} & \mathbf{I} \\ -\mathbf{M}^{-1}\mathbf{K} & -\mathbf{M}^{-1}\mathbf{D} \end{pmatrix}, \quad \mathbf{B}_1 = \begin{pmatrix} \mathbf{0} \\ \mathbf{M}^{-1}\mathbf{G}_1 \end{pmatrix}, \quad \mathbf{B}_2 = \begin{pmatrix} \mathbf{0} \\ \mathbf{M}^{-1}\mathbf{G}_2 \end{pmatrix} \tag{3.2a}$$

and an additional disturbance v' independent of α has been introduced for greater flexibility of the formulation. We assume that (3.2) has measured output variables y and controlled output variables z:

$$\begin{aligned} y &= \mathbf{C}_1 x + w, \\ z &= \mathbf{C}_2 x \end{aligned} \tag{3.3}$$

and that $\boldsymbol{v}$, $\boldsymbol{v}'$, and $\boldsymbol{w}$ are uncorrelated white noise processes with intensities $\mathbf{Q}_v$, $\mathbf{V}$, and $\mathbf{Q}_w$, respectively.

In the remainder of this paper, the total mass of the structure is assumed to represent the structural criterion J_s. Thus, for a structure consisting of n_a one-dimensional finite elements, each having a cross-sectional area α_i, length l_i and density ρ:

$$J_s = \sum_i^{n_a} \rho l_i \alpha_i. \tag{3.4}$$

For the control criterion J_c associated with (3.2) and (3.3), we assume the LQG index

$$J_c = \lim_{t \to \infty} \mathrm{E}\{z^T(t)\mathbf{D}_o z(t) + \boldsymbol{u}^T(t)\mathbf{R}\boldsymbol{u}(t)\} \tag{3.5}$$

where E is the expectation, $\mathbf{D}_o$ is a non-negative definite weighting matrix which could have an explicit dependence on $\boldsymbol{\alpha}$, and $\mathbf{R}$ is positive definite. This would arise, for instance, if the first term in (3.5) were to represent the total energy in the system with $z = (r, \dot{r})^T$ and $\mathbf{D}_o = \mathrm{diag}(\mathbf{K}, \mathbf{M})$. Without loss of generality, in the sequel we will take $z = x$. Under standard assumptions of stabilizability and detectability, the optimal compensator C^* for (3.5) is implemented (Kwakernaak and Sivan (1972)) by:

$$\begin{aligned} \boldsymbol{u}_o &= -\mathbf{R}^{-1}\mathbf{B}_1^T\mathbf{P}x_o \\ \dot{x}_o &= (\mathbf{A} - \mathbf{K}_f\mathbf{C})x_o + \mathbf{K}_f y + \mathbf{B}_1\boldsymbol{u}_o, \end{aligned} \tag{3.6}$$

and the optimal cost J_c associated with this compensator is

$$J_c(C) = \mathrm{tr}\{\mathbf{P}(\mathbf{B}_2\mathbf{Q}_v B_2^T + \mathbf{V}) + \mathbf{P}_f\mathbf{P}\mathbf{B}_1\mathbf{R}^{-1}\mathbf{B}_1^T\mathbf{P}\}. \tag{3.7}$$

where $\mathbf{P}$ and $\mathbf{P}_f$ are the unique positive definite solutions to the algebraic Riccati equations

$$\begin{aligned} \mathrm{G}_1(\boldsymbol{\alpha}, \mathbf{P}, \mathbf{P}_f) &= \mathbf{A}^T\mathbf{P} + \mathbf{P}\mathbf{A} + \mathbf{D}_o - \mathbf{P}\mathbf{B}_1\mathbf{R}^{-1}\mathbf{B}_1^T\mathbf{P} = 0, \\ \mathbf{G}_2(\boldsymbol{\alpha}, \mathbf{P}, \mathbf{P}_f) &= \mathbf{A}\mathbf{P}_f + \mathbf{P}_f\mathbf{A}^T + \mathbf{B}_2\mathbf{Q}_v\mathbf{B}_2^T + \mathbf{V} - \mathbf{P}_f\mathbf{C}_1^T\mathbf{Q}_w^{-1}\mathbf{C}_1\mathbf{P}_f = 0 \end{aligned} \tag{3.8}$$

and

$$\boldsymbol{K}_f = \mathbf{P}_f\mathbf{C}_1^T\mathbf{Q}_w^{-1}.$$

With the above representation for J_c, we seek the optimality conditions for

$$\min_{\boldsymbol{\alpha}} J_\lambda(\boldsymbol{\alpha}) = (1-\lambda)J_s(\boldsymbol{\alpha}) + \langle \boldsymbol{v}, \boldsymbol{\alpha} \rangle + \lambda\,\mathrm{tr}\{\mathbf{P}(\mathbf{B}_2\mathbf{Q}_v\mathbf{B}_2^T + \mathbf{V}) + \mathbf{P}_f\mathbf{P}\mathbf{B}_1\mathbf{R}^{-1}\mathbf{B}_1^T\mathbf{P}\} \tag{3.9}$$

subject to the constraints $[\mathbf{G}_1, \mathbf{G}_2] = \mathbf{G}(\alpha, \mathbf{P}, \mathbf{P}_f) = \mathbf{0}$ of (3.8). In (3.9) in n_a-dimensional vector $\boldsymbol{v} \in R^{na}$ has been introduced to "regularize" the problem and to serve the purpose of initializing the homotopy path.

Assumption A. *For every $\alpha \in \bar{D}$ (the closure of D), G_1 and G_2 have unique positive definite solutions. These conditions are satisfied if the open loop system possesses damping, or more generally, if the system is stabilizable and observable for each $\boldsymbol{\alpha}$.*

Let $\boldsymbol{\Sigma}_+$ denote the set of symmetric $n_x \times n_x$ positive definite matrices. Fix $\lambda \in [0, 1]$ and define $f: R^{n_a} \times \boldsymbol{\Sigma}_+ \times \boldsymbol{\Sigma}_+ \to R$ by

$$f(\boldsymbol{\alpha}, \mathbf{P}, \mathbf{P}_f) = (1-\lambda)J_s(\boldsymbol{\alpha}) + \langle \boldsymbol{v}, \boldsymbol{\alpha} \rangle + \lambda\,\mathrm{tr}\{\mathbf{P}(\mathbf{B}_2\mathbf{Q}_v\mathbf{B}_2^T + \mathbf{V}) + \mathbf{P}_f\mathbf{P}\mathbf{B}_1\mathbf{R}^{-1}\mathbf{B}_1^T\mathbf{P}\}. \tag{3.10}$$

The optimization problem (3.9) is then equivalent to

$$\min_{\boldsymbol{\alpha}, \mathbf{P}, \mathbf{P}_f} f(\boldsymbol{\alpha}, \mathbf{P}, \mathbf{P}_f) \quad \text{subject to} \quad \mathbf{G}(\boldsymbol{\alpha}, \mathbf{P}, \mathbf{P}_f) = 0. \tag{3.11}$$

The local condition for optimality is contained in

Proposition 3.1. Suppose Assumption A holds and that $(\boldsymbol{\alpha}^*, \mathbf{P}^*, \mathbf{P}_f^*)$ is a local extremum for (3.11). Then there exist unique matrices $\mathbf{Z}_1, \mathbf{Z}_2 \in \boldsymbol{\Sigma}_+$ such that

$$0=(1-\lambda)\frac{\partial J_s}{\partial \alpha_i}+v_i+\lambda\,\mathrm{tr}\left\{\mathbf{P}\frac{\partial(\mathbf{B}_2\mathbf{Q}_v\mathbf{B}_2^T+\mathbf{V})}{\partial\alpha_i}+\mathbf{P}\mathbf{P}_f\mathbf{P}\frac{\partial(\mathbf{B}_1\mathbf{R}^{-1}\mathbf{B}_1^T)}{\partial\alpha_i}\right.$$
$$+\mathbf{Z}_1\left[\frac{\partial\mathbf{A}^T}{\partial\alpha_i}\mathbf{P}+\mathbf{P}\frac{\partial\mathbf{A}}{\partial\alpha_i}+\frac{\partial\mathbf{D}_o}{\partial\alpha_i}-\mathbf{P}\frac{\partial(\mathbf{B}_1\mathbf{R}^{-1}\mathbf{B}_1^T)}{\partial\alpha_i}\mathbf{P}\right]$$
$$\left.+\mathbf{Z}_2\left[\frac{\partial\mathbf{A}}{\partial\alpha_i}\mathbf{P}_f+\mathbf{P}_f\frac{\partial\mathbf{A}^T}{\partial\alpha_i}+\frac{\partial(\mathbf{B}_2\mathbf{Q}_v\mathbf{B}_2^T+\mathbf{V})}{\partial\alpha_i}-\mathbf{P}_f\frac{\partial(\mathbf{C}_1^T\mathbf{Q}_w^{-1}\mathbf{C}_1)}{\partial\alpha_i}\mathbf{P}_f\right]\right\},\quad i=1,\dots n_a \tag{3.12a}$$

$$0=(\mathbf{A}-\mathbf{B}_1\mathbf{R}^{-1}\mathbf{B}_1^T\mathbf{P})\mathbf{Z}_1+\mathbf{Z}_1(\mathbf{A}^T-\mathbf{P}\mathbf{B}_1\mathbf{R}^{-1}\mathbf{B}_1^T)$$
$$+\mathbf{B}_2\mathbf{Q}_v\mathbf{B}_2^T+\mathbf{V}+\mathbf{P}_f\mathbf{P}\mathbf{B}_1\mathbf{R}^{-1}\mathbf{B}_1^T+\mathbf{B}_1\mathbf{R}^{-1}\mathbf{B}_1^T\mathbf{P}\mathbf{P}_f \tag{3.12b}$$
$$0=(\mathbf{A}^T-\mathbf{C}_1^T\mathbf{Q}_w^{-1}\mathbf{C}_1\mathbf{P}_f)\mathbf{Z}_2+\mathbf{Z}_2(\mathbf{A}-\mathbf{P}_f\mathbf{C}_1^T\mathbf{Q}_w^{-1}\mathbf{C}_1)+\mathbf{P}\mathbf{B}_1\mathbf{R}^{-1}\mathbf{B}_1^T\mathbf{P}. \tag{3.12c}$$

Proof. Suppose ($\boldsymbol{\alpha}^*$, $\mathbf{P}^*$, $\mathbf{P}_f^*$) is a local extremum. We first verify that the problem is regular, that is, the differential $\mathbf{G}_*$ of $\mathbf{G}$ has full rank at $(\boldsymbol{\alpha}^*,\mathbf{P}^*,\mathbf{P}_f^*)$. Noting that

$$\mathbf{G}_*:R^{n_a}\times R^{n_x(n_x+1)/2}\times R^{n_x(n_x+1)/2}\to R^{n_x(n_x+1)/2}\times R^{n_x(n_x+1)/2}$$

it is sufficient to verify that G_* restricted to $R^{n_x(n_x+1)/2}\times R^{n_x(n_x+1)/2}$ is invertible. By direct computation we determine that at $\boldsymbol{\alpha}^*,\mathbf{P}^*$

$$\frac{\partial\mathbf{G}_1}{\partial\mathbf{P}}:\mathbf{S}_1\to\mathbf{A}^T(\boldsymbol{\alpha}^*)\mathbf{S}_1+S_1\mathbf{A}(\boldsymbol{\alpha}^*)-\mathbf{S}_1\mathbf{B}_1(\boldsymbol{\alpha}^*)\mathbf{R}^{-1}\mathbf{B}_1^T(\boldsymbol{\alpha}^*)\mathbf{P}^*-\mathbf{P}^*\mathbf{B}_1(\boldsymbol{\alpha}^*)\mathbf{R}^{-1}\mathbf{B}_1^T(\boldsymbol{\alpha}^*)\mathbf{S}_1$$

for any $\mathbf{S}_1\in\boldsymbol{\Sigma}$. Note that $\mathbf{A}(\boldsymbol{\alpha}^*)-\mathbf{B}_1(\boldsymbol{\alpha}^*)\mathbf{R}^{-1}\mathbf{B}_1(\boldsymbol{\alpha}^*)\mathbf{P}^*$ is a stable matrix. So by the uniqueness of the solution of the Lyapunov equation that $\mathbf{S}_1$ solves when $\partial\mathbf{G}_1/\partial\mathbf{P}(\mathbf{S}_1)$ vanishes, it follows that $\mathbf{S}_1$ vanishes. Hence, $\partial\mathbf{G}_1/\partial\mathbf{P}$ is one to one. In a similar manner we can verify that $\partial\mathbf{G}_2/\partial\mathbf{P}_f$ is also one to one, and thereby establish that $\mathbf{G}_*$ is onto.

Having established regularity of the problem it follows that ($\boldsymbol{\alpha}^*$, $\mathbf{P}^*$, $\mathbf{P}_f^*$) is a stationary point of the Lagrangian L,

$$L=f+\gamma G,$$

where $\gamma:\boldsymbol{\Sigma}\times\boldsymbol{\Sigma}\to R$ denotes the Lagrange multiplier. It is straightforward to show that there exists a unique pair of matrices $\mathbf{Z}_1,\mathbf{Z}_2\in\boldsymbol{\Sigma}$ such that

$$\gamma(\mathbf{S}_1,\mathbf{S}_2)=\mathrm{tr}\{\mathbf{Z}_1\mathbf{S}_1+\mathbf{Z}_2\mathbf{S}_2\}\quad\text{for all}\quad\mathbf{S}_1,\mathbf{S}_2\in\boldsymbol{\Sigma}.$$

At the stationary point all of the partial derivatives of L must vanish. Hence, $\partial L/\partial\mathbf{P}_f$ must vanish. This implies that

$$\mathrm{tr}\{(\mathbf{P}\mathbf{B}_1\mathbf{R}^{-1}\mathbf{B}_1^T\mathbf{P}+\mathbf{Z}_2(\mathbf{A}-\mathbf{P}_f\mathbf{C}_1^T\mathbf{Q}_w^{-1}\mathbf{C}_1)+(\mathbf{A}^T-\mathbf{C}_1^T\mathbf{Q}_w^{-1}\mathbf{C}_1\mathbf{P}_f)\mathbf{Z}_2)\mathbf{S}_2\}=0$$

for all $\mathbf{S}_2\in\boldsymbol{\Sigma}$. A sufficient condition for this is for $\mathbf{Z}_2$ to satisfy the Lyapunov Eq. (3.12c). A similar argument establishes (3.12b). Finally, the equations in (3.12a) are derived from $\partial L/\partial\alpha_i=0$, $i=1,\dots,n_a$. □

Thus for the LQG formulation, the necessary conditions involve solving two algebraic Riccati Eqs. (3.8), two Lyapunov Eqs. (3.12b, c) and a gradient Eq. (3.12a) for α_i, $i=1,\dots,n_a$. The LQR optimality conditions are recovered by eliminating equations and terms involving $\mathbf{Z}_2$ and $\mathbf{P}_f$. Specifically, these optimality conditions are the zeros of the function $\mathbf{H}$: $R\times R^{na}\times\boldsymbol{\Sigma}_+\times\boldsymbol{\Sigma}_+\to R^{na}\times\boldsymbol{\Sigma}_+\times\boldsymbol{\Sigma}_+$ defined by $\mathbf{H}=[\mathbf{H}_1,\mathbf{H}_2,\mathbf{H}_3]$ which involve one gradient equation for α_i, $i=1,\dots,n_a$, one Lyapunov equation, and one Riccati equation;

$$\mathbf{H}_1(\lambda,\boldsymbol{\alpha},\mathbf{Z},\mathbf{P})=(1-\lambda)\frac{\partial J_s}{\partial\alpha_i}+v_i+\lambda\,\mathrm{tr}\left\{\mathbf{P}\frac{\partial(\mathbf{B}_2\mathbf{Q}_v\mathbf{B}_2^T+\mathbf{V})}{\partial\alpha_i}\right.$$
$$\left.+\mathbf{Z}\left[2\mathbf{P}\frac{\partial\mathbf{A}}{\partial\alpha_i}+\frac{\partial\mathbf{D}_o}{\partial\alpha_i}-\mathbf{P}\frac{\partial(\mathbf{B}_1\mathbf{R}^{-1}\mathbf{B}_1^T)}{\partial\alpha_i}\mathbf{P}\right]\right\};\quad i=1,\dots,n_a \tag{3.13a}$$

$$\mathbf{H}_2(\lambda, \boldsymbol{\alpha}, \mathbf{Z}, \mathbf{P}) = \mathbf{A}_c\mathbf{Z} + \mathbf{Z}\mathbf{A}_c^T + \mathbf{B}_2\mathbf{Q}_p\mathbf{B}_2^T + \mathbf{V}, \tag{3.13b}$$

$$\mathbf{H}_3(\lambda, \boldsymbol{\alpha}, \mathbf{Z}, \mathbf{P}) = \mathbf{A}^T\mathbf{P} + \mathbf{P}\mathbf{A} + \mathbf{D}_o - \mathbf{P}\mathbf{B}_1\mathbf{R}^{-1}\mathbf{B}_1^T\mathbf{P}, \tag{3.13c}$$

with $\mathbf{A}_c = \mathbf{A} - \mathbf{B}_1\mathbf{R}^{-1}\mathbf{B}_1^T\mathbf{P}$.

We note that after averaging over initial conditions, it can be shown that (3.13) is equivalent to the equations derived in (Salama et al. 1988), but require fewer Lyapunov equations to implement (one versus n_a).

4 Homotopy strategy

For all $\lambda \in [0,1]$, our goal is to minimize (3.9) in the case of the LQG formulation or it's LQR equivalent (where $\mathbf{P}_f = 0$) by finding the design variables α that satisfy the corresponding optimality conditions (3.12) or (3.13). The basic strategy is: given the solution at a value λ_o, smoothly propagate it to a new solution at $\lambda_o \to \Delta\lambda$ via some local mechanism such as a Newton method or iterative optimization. This strategy has been analyzed in detail by Milman et al. (1990). In the following, only a summary of the results is given assuming the LQR formulation.

Let x denote a generic point $(\boldsymbol{\alpha}, \mathbf{Z}, \mathbf{P}) \in R^{n_a} \times \Sigma_+ \times \Sigma_+$ so that $\mathrm{H}(\lambda, x)$ stands for $\mathbf{H}(\lambda, \boldsymbol{\alpha}, \mathbf{Z}, \mathbf{P})$. In determining the zeros of H, the following proposition asserts that in a small neighborhood about the optimal at $\lambda = 0$, there is a smooth path parameterized by λ consisting of the global optimal solution. The proof is included in the Appendix.

Proposition 4.1. Suppose that min $J_s(\boldsymbol{\alpha})$ has a unique global solution α^* satisfying the second order sufficiency condition on the positivity of the Hessian $[J_s(\boldsymbol{\alpha}^*)]_{,\alpha_i\alpha_j} > 0$. Further, assume that J_s is coercive so that $|J_s(\boldsymbol{\alpha})| \to \infty$ as $|\boldsymbol{\alpha}| \to \infty$. Then there exists $\varepsilon > 0$ such that (3.9) has a unique global solution for $\lambda < \varepsilon$.

The next proposition provides a sufficient condition for the path to remain locally optimal. It's proof is contained in (Milman et al. 1990).

Proposition 4.2. Let $\phi(\lambda) = (\lambda, x(\lambda))$ denote a smooth path in $[0,r) \times R^{n_a} \times \Sigma_+ \times \Sigma_+$ with $\mathbf{H}(\phi(\lambda)) = 0$ and $\mathbf{H}_{,x}$ invertible for $\lambda \in [0,r)$. Such an r is guaranteed by Proposition 4.1. Then $\boldsymbol{\alpha}(\lambda)$ is a local minimum for J_λ for each $\lambda \in [0,r)$.

The purpose of the following lemma is to demonstrate that the zero set of H is "generically" well-behaved.

Lemma 4.3. *Suppose that* $\mathbf{H}(0,x) = 0$ *has a unique solution. Then for almost every choice of* $v \in R^{n_a}$*, the solution path emanating from* $(0, x^*)$ *is diffeomorphic to the real line R.*

The main point of this lemma (which is proved in the Appendix) is to demonstrate that, at least topologically, the zero set of **H** is well-behaved in a generic sense ("with probability one"). Thus, following the path defined by one of the zero curves of **H**, not just the one emanating from the optimal at $\lambda = 0$, will not lead to a pathological behavior such as bifurcations or curves with infinite length in bounded sets. Another fundamental and generally difficult question that arises when employing homotopy methods is whether or not the path remains bounded. The following result provides a partial answer to this question.

Theorem 4.4. *Suppose that* J_s, $\mathbf{B}_i$, $\mathbf{D}_o$, *and* $\mathbf{A}$ *are all polynomials in* $\alpha_1, \ldots, \alpha_{n_a}$, *and assume coercivity of* $J_s(\boldsymbol{\alpha})/|\boldsymbol{\alpha}|$. *If* $\mathbf{H}(0,x) = 0$ *has a unique solution, then for any* $\varepsilon > 0$ *and for almost every* $v \in R^{n_a}$ *the component of* $H^{-1}(0)$ *containing* $(0, x^*)$ *can be continued to* $\lambda = 1 - \varepsilon$ *and is a bounded set in* $\boldsymbol{\Omega} = [0, 1-\varepsilon] \times R^{n_a} \times \Sigma_+ \times \Sigma_+$.

The proof of Theorem 4.4 in the Appendix contains a number of important points. First, it shows that if any component of $\mathbf{H}^{-1}(0)$ is nondegenerate in the sense that there exists at least one point in the component where $\partial\mathbf{H}/\partial x$ is invertible, then that component is also a bounded set in $\boldsymbol{\Omega}$. This observation is relevant to the problem of finding Pareto optimal solution where it may be necessary to follow paths other than the one emanating from $(0, x^*)$. The "ε" appears in the theorem because the cost functional makes it possible for $\boldsymbol{\alpha}(\lambda)$ to become unbounded in a neighborhood of one. The coercivity assumption in the theorem can be relaxed to $\lim_{|\alpha|\to\infty} [J_s(\boldsymbol{\alpha}) - \langle \boldsymbol{\nu}, \boldsymbol{\alpha} \rangle] \to \infty$ without modifying the proof. With regards to the hypothesis of polynomial dependence on the design parameters it should be observed that these conditions hold for an arbitrary Taylor expansion of the system matrices about an initial design.

A slight generalization of Theorem 4.4 can be derived for systems arising from finite element models which typically have a polynomial dependence on the design parameter in their mass, damping and stiffness matrices (Milman et al. 1990).

In the next proposition, we state the conditions under which the solution $\mathbf{H}(\lambda, x) = 0$ remains stable if the data of the problem are slightly perturbed. The proof is contained in (Milman et al. 1990).

Proposition 4.5. Let $\mathbf{F}(t, \lambda, x)$ denote a family of functions parameterized by $t \in (-\beta, \beta)$ such that $\mathbf{F}(0, \lambda, x) = \mathbf{H}(\lambda, x)$ and $\mathbf{F}(.,.,.)$ is twice continuously differentiable. Let $\mathbf{G} = \mathbf{H}^{-1}(0) \cap \Omega$ (cf. Theorem 4.4) and let B denote a closed bounded set containing G. Then given $\varepsilon' > 0$ there exists $\delta > 0$ such that

(i) If $|t_0| < \delta$, then any solution (λ, x) of $\mathbf{F}(t_0, \lambda, x) = 0$ in B has the property that the distance $d(\mathbf{G}, (\lambda, x)) < \varepsilon'$.

(ii) There exists an open set $\mathbf{T}(\mathbf{G}) \supset \mathbf{G}$ such that $\mathbf{F}(t,.,.)|\mathbf{T}(\mathbf{G})$ has no critical points; that is, for each t with $|t| < \delta, \mathbf{F}(t,.,.)^{-1}(0) \cap \mathbf{T}(\mathbf{G})$ is a one-dimensional manifold.

(iii) Given any $(\lambda^*, x^*) \in \mathbf{G}$ there exists $\delta(\lambda^*, x^*) > 0$ such that $\mathbf{F}(t, \lambda, x) = 0$ has a solution (λ_t, x_t) for each t with $|t| < \delta(\lambda^*, x^*)$ and $d((\lambda_t, x_t), (\lambda^*, x^*)) < \varepsilon'$.

Several of the theorems and propositions above assume that the structural objective $J_s(\boldsymbol{\alpha})$ is a convex and coercive function of the design variables $\boldsymbol{\alpha}$. These conditions are easily met when J_s represents the mass of the structure and $\boldsymbol{\alpha}$ represents cross sectional areas. In more general cases (e.g. when $\boldsymbol{\alpha}$ represents shape design variables) these conditions may not be satisfied, and the theorems above may require modifications. A possible way for circumventing nonconvex problems in shape optimization is to initially seek (i.e. for small values of λ) optimal shapes in the vicinity of a nominal a priori known configuration. A way to fit this into the current framework is to introduce a quadratic form of a structural cost J_s which is uniquely minimized by the desired nominal configuration, thereby restoring the convexity of the problem.

5 Newton methods

Numerous approaches have been proposed for solving parameterized systems of the form

$$G(\boldsymbol{\alpha}, \lambda) = 0 \tag{5.1}$$

where λ may be a multidimensional parameter and G is a smooth mapping from some function space S into itself $(\boldsymbol{\alpha} \in S, G(\boldsymbol{\alpha}, \lambda) \in S)$. In our case G is derived by the differentiation

$$G(\boldsymbol{\alpha}, \lambda) = \frac{\partial}{\partial \boldsymbol{\alpha}} J_\lambda(\boldsymbol{\alpha}) \tag{5.2}$$

where $J_\lambda(\boldsymbol{\alpha})$ is given by (3.9) in terms of a one-dimensional parameter $\lambda \in [0, 1]$. Then $G(\boldsymbol{\alpha}, \lambda)$ denotes an n_a-dimensional vector with components $G(\boldsymbol{\alpha}, \lambda)^{(i)}$, $(i \in \{1, 2, \ldots, n_a\})$. Correspondingly, $\frac{\partial G(\boldsymbol{\alpha}, \lambda)}{\partial \boldsymbol{\alpha}}$ denotes on $n_a \times n_a$ matrix whose (i,j)-component will be denoted by $\frac{\partial G(\boldsymbol{\alpha}, \lambda)^{(i,j)}}{\partial \boldsymbol{\alpha}}$ $(i, j \in \{1, 2, .., n_a\})$, and $\frac{\partial G(\boldsymbol{\alpha}, \lambda)}{\partial \lambda}$ denotes an n_a-dimensional vector with components $\frac{\partial G(\boldsymbol{\alpha}, \lambda)^{(i)}}{\partial \lambda}$ $(i \in \{1, \ldots, n_a\})$.

Under suitable regularity conditions, the system (5.1) determines $\boldsymbol{\alpha}(\lambda)$ where $\boldsymbol{\alpha}$ is now parameterized by λ (Keller 1987). In some cases one may be interested only in the solution α for a particular value of λ. There, global homotopy methods can be used (Keller 1987; Watson 1986).

But because the zeros of the system (5.2) are relevant for a continuum of values, global homotopy methods cannot be used here.

Newton methods have several advantages when approximations for $\boldsymbol{\alpha}$ are desired over some range of the parameter since the underlying smooth structure of the problem as well as the usefulness of nearby parameterized values can be exploited. Thus we suppose first that $\boldsymbol{\alpha}_{[0]} = \boldsymbol{\alpha}(\lambda_0)$ has been determined for $\lambda = \lambda_0$, and consider the solution $\boldsymbol{\alpha}_{[1]} = \boldsymbol{\alpha}(\lambda_1)$ for a nearby value of the parameter. Then subject to suitable regularity conditions the iteration.

$$\begin{aligned}
\boldsymbol{\alpha}_{[1]}^{(0)} &= \boldsymbol{\alpha}_{(0)} - (\lambda_1 - \lambda_0)\frac{\partial \boldsymbol{G}(\boldsymbol{\alpha}_{[0]}, \lambda_0)}{\partial \boldsymbol{\alpha}}^{-1}\frac{\partial \boldsymbol{G}(\boldsymbol{\alpha}_{[0]}, \lambda_0)}{\partial \lambda} \\
\boldsymbol{\alpha}_{[1]}^{(k+1)} &= \boldsymbol{\alpha}_{[1]}^{(k)} + \boldsymbol{\Delta}_{[1]}^{(k)} \quad (k \in \{0, 1, 2, \ldots\}) \\
\boldsymbol{\Delta}_{[1]}^{(k)} &= -\frac{\partial \boldsymbol{G}(\boldsymbol{\alpha}_{[1]}^{(k)}, \lambda_1)}{\partial \boldsymbol{\alpha}}^{-1} \boldsymbol{G}(\boldsymbol{\alpha}_{[1]}^{(k)}, \lambda_1)
\end{aligned} \tag{5.3}$$

will converge quadratically (Keller 1987) to λ_1(i.e., $\lim_{k\to\infty} \boldsymbol{\alpha}_{[1]}^{(k)} = \boldsymbol{\alpha}_{[1]}$).

Variations can be implemented according to the nature of the problem. For example, the non-invertibility of $\frac{\partial \boldsymbol{G}}{\partial \boldsymbol{\alpha}}$, which can occur at a fold, at a bifurcation point or at a limit point, can sometimes be circumvented by a different parameterization of the problem (e.g., an arclength parameterization as discussed in (Keller 1987)). Another possibility is that the matrix can be made invertible by the addition of a suitably chosen positive definite matrix. Then even if the iteration diverges, the step $\boldsymbol{\Delta}_{[1]}^{(k)}$ can be used as inputs to line search routines (Fletcher 1987) for the optimization of $J_\lambda(\boldsymbol{\alpha})$.

To simplify the analysis we restrict the consideration here to the LQR formulation of the optimality conditions summarized in (3.13). We also assume the conditions of Propositions 4.1 and 4.2 so as to assure the well-posedness of the continuation process. Therefore, for the LQR formulation

$$J(\boldsymbol{\alpha}, \lambda) = (1-\lambda)J_s(\boldsymbol{\alpha}) + \langle \boldsymbol{\nu}, \boldsymbol{\alpha} \rangle + \lambda \operatorname{tr}\{\mathbf{P}(\mathbf{B}_2\mathbf{Q}_v\mathbf{B}_2^T + \mathbf{V})\} \tag{5.4a}$$

$$\mathbf{A}^T\mathbf{P} + \mathbf{P}\mathbf{A} + \mathbf{D}_o - \mathbf{P}\mathbf{B}_1\mathbf{R}^{-1}\mathbf{B}_1^T\mathbf{P} = 0. \tag{5.4b}$$

Now the Riccati Eq. (5.4b) can be formally inverted to determine $\mathbf{P}$ as a function of the parameters of the system:

$$\mathbf{P} = \mathbf{F}(\mathbf{A}, \mathbf{D}_o, \mathbf{B}_1\mathbf{R}^{-1}\mathbf{B}_1^T). \tag{5.5}$$

Then the function $J(\boldsymbol{\alpha}, \lambda)$ in (5.4a) can be treated as a function of $\boldsymbol{\alpha}$ and λ. From (5.2) and (5.4a) we have

$$\boldsymbol{G}(\boldsymbol{\alpha}, \lambda)^{(i)} = (1-\lambda)\frac{\partial J_s(\boldsymbol{\alpha})}{\partial \alpha_i} + \boldsymbol{\nu} + \lambda \operatorname{tr}\left\{\frac{\partial \mathbf{P}}{\partial \alpha_i}(\mathbf{B}_2\mathbf{Q}_v\mathbf{B}_2^T + \mathbf{V}) + \mathbf{P}\frac{\partial(\mathbf{B}_2\mathbf{Q}_v\mathbf{B}_2^T + \mathbf{V})}{\partial \alpha_i}\right\} \tag{5.6a}$$

$$\begin{aligned}
\frac{\partial \boldsymbol{G}(\boldsymbol{\alpha}, \lambda)^{(i,j)}}{\partial \boldsymbol{\alpha}} &= (1-\lambda)\frac{\partial^2 J_s(\boldsymbol{\alpha})}{\partial \alpha_i \partial \alpha_j} + \lambda \operatorname{tr}\left\{\frac{\partial^2 \mathbf{P}}{\partial \alpha_i \partial \alpha_j}(\mathbf{B}_2\mathbf{Q}_v\mathbf{B}_2^T + \mathbf{V}) + \frac{\partial \mathbf{P}}{\partial \alpha_i}\frac{\partial(\mathbf{B}_2\mathbf{Q}_v\mathbf{B}_2^T + \mathbf{V})}{\partial \alpha_j}\right. \\
&\quad \left. + \frac{\partial \mathbf{P}}{\partial \alpha_j}\frac{\partial(\mathbf{B}_2\mathbf{Q}_v\mathbf{B}_2^T + \mathbf{V})}{\partial \alpha_i} + \mathbf{P}\frac{\partial^2(\mathbf{B}_2\mathbf{Q}_v\mathbf{B}_2^T + \mathbf{V})}{\partial \alpha_i \partial \alpha_j}\right\}
\end{aligned} \tag{5.6b}$$

$$\frac{\partial \boldsymbol{G}(\boldsymbol{\alpha}, \lambda)^{(i)}}{\partial \lambda} = -\frac{\partial J_s(\boldsymbol{\alpha})}{\partial \alpha_i} + \operatorname{tr}\left\{\frac{\partial \mathbf{P}}{\partial \alpha_i}(\mathbf{B}_2\mathbf{Q}_v\mathbf{B}_2^T + \mathbf{V}) + \mathbf{P}\frac{\partial(\mathbf{B}_2\mathbf{Q}_v\mathbf{B}_2^T + \mathbf{V})}{\partial \alpha_i}\right\}. \tag{5.6c}$$

To determine the $\boldsymbol{\alpha}$-derivatives of $\mathbf{P}$, it is necessary to differentiate (5.4b). As in (3.13), we define

$$\mathbf{A}_c = \mathbf{A} - \mathbf{B}_1\mathbf{R}^{-1}\mathbf{B}_1^T\mathbf{P}. \tag{5.7}$$

Then differentiation of (5.4b) gives

$$\mathbf{A}_c^T \frac{\partial \mathbf{P}}{\partial \alpha_i} + \frac{\partial \mathbf{P}}{\partial \alpha_i} \mathbf{A}_c + \mathbf{S}_1^{(i)} = 0 \tag{5.8a}$$

$$\mathbf{S}_1^{(i)} = \frac{\partial \mathbf{A}^T}{\partial \alpha_i} \mathbf{P} + \mathbf{P} \frac{\partial \mathbf{A}}{\partial \alpha_i} - \mathbf{P} \frac{\partial (\mathbf{B}_1 \mathbf{R}^{-1} \mathbf{B}_1^T)}{\partial \alpha_i} \tag{5.8b}$$

for $i \in \{1, 2, \ldots, n_a\}$. The Lyapunov equations (5.8a) can be formally inverted to give:

$$\frac{\partial \mathbf{P}}{\partial \alpha_i} = \mathscr{L}(\mathbf{A}_c, \mathbf{S}_1^{(i)}) \tag{5.9}$$

where the Lyapunov solution can be written explicitly as (Kwakernaak and Sivan (1972)):

$$\mathscr{L}(\mathbf{A}_c \mathbf{S}_1^{(i)}) = \int_0^\infty \exp(\mathbf{A}_c^T t) \mathbf{S}_1^{(i)} \exp(\mathbf{A}_c t)\, \mathrm{d}t. \tag{5.10}$$

It is worthwhile to note (as in the proof of Proposition 4.2) that the expression for the right-hand side of (5.6a) can be simplified by exploiting the properties of the trace operator:

$$\begin{aligned} \operatorname{tr}\left\{ \frac{\partial \mathbf{P}}{\partial \alpha_i} (\mathbf{B}_2 \mathbf{Q}_v \mathbf{B}_2^T + \mathbf{V}) \right\} &= \operatorname{tr}\{\mathscr{L}(\mathbf{A}_c, \mathbf{S}_1^{(i)})(\mathbf{B}_2 \mathbf{Q}_v \mathbf{B}_2^T + \mathbf{V})\} \\ &= \int_0^\infty \operatorname{tr}\{\exp(\mathbf{A}_c^T t) \mathbf{S}_1^{(i)} \exp(\mathbf{A}_c t)(\mathbf{B}_2 \mathbf{Q}_v \mathbf{B}_2^T + \mathbf{V})\} dt \\ &= \int_0^\infty \operatorname{tr}\{\exp(\mathbf{A}_c t)(\mathbf{B}_2 \mathbf{Q}_v \mathbf{B}_2^T + \mathbf{V}) \exp(\mathbf{A}_c^T t) \mathbf{S}_1^{(i)}\} dt \\ &= \operatorname{tr}\{\mathscr{L}(\mathbf{A}_c^T, \mathbf{B}_2 \mathbf{Q}_v \mathbf{B}_2^T + \mathbf{V}) \mathbf{S}_1^{(i)}\}. \end{aligned} \tag{5.11}$$

Thus, the computation of the n_a components of $G(\boldsymbol{\alpha}, \lambda)$ requires the solution of one Riccati equation as given by (5.6c) and one Lyapunov equation as given in (5.11). The computation of $\frac{\partial G}{\partial \lambda}$ as given by (5.5c) requires the solution of no additional algebraic equations; however, the computation $\frac{\partial \mathbf{G}}{\partial \boldsymbol{\alpha}}$ as given by (5.6b) will require the solution of the n_a Lyapunov equations for the $\frac{\partial \mathbf{P}}{\partial \alpha_i}$ as given by (5.9). The details of this procedure are given in (Milman et al. 1990).

6 Numerical results

The numerical experiments described in this section demonstrate the results of the foregoing theory. Three prototype examples are used; all employing the LQR formulation. Implementation of the homotopy strategy of Sect. 4 is achieved by iterative optimization in the first two examples, and by Newton's method in the last example.

Iterative optimization. In this approach, the homotopy parameter λ starts at $\lambda = 0$ with $\alpha_1, \ldots, \alpha_{na}$ initialized to a predetermined sufficiently small allowable size $\boldsymbol{\alpha}_0$. At this point in the solution space, J_λ is fully weighted toward minimizing J_s only. Then by minimizing J_{λ_0} one obtains $\boldsymbol{\alpha}_0^*$ for which $\mathbf{H}(\lambda_0, x_0^*) = 0$. For the next iteration and for every succeeding one, λ is incremented and the weighting is shifted gradually toward J_c. For a typical iteration j, the following steps are performed:

(i) $\lambda_j \Leftarrow \lambda_{j-1} + \Delta\lambda_{j-1}$

(ii) Initialize the minimization of $J_{\lambda j}$ by using $\boldsymbol{\alpha}_j \Leftarrow \alpha^*_{j-1}$. This will result in $\boldsymbol{\alpha}^*_j$ for which conditions (3.13) hold.

In performing the minimization in (ii) above, we employed the Automated Design Synthesis (ADS) system of general purpose subroutines (Vanderplaats 1984). ADS provides a wide selection of options at three levels: strategy, optimization, and line search. Available strategies include sequential linear and quadratic programming, and sequential unconstrained minimization coupled with various penalty methods. At the optimization level, one can choose between the Fletcher–Reeves algorithm and the variable metric method of Broydon–Fletcher–Goldfarb–Shanno (BFGS) for unconstrained minimization, or Zoutendijk's method of feasible directions and modifications thereof for constrained minimization. For one-dimensional line search, the options include a combination of polynomial interpolation/extrapolation, solution bounding, and the method of Golden Section. Not all combination of options are compatible at the three levels, and the program parameters must be adjusted to suit the problem at hand. For this purpose, an analytical function was contrived which possessed such features as: easy to compute closed form solution, multiple minima, and insensitivity of the functions gradient near the minima to design parameters. Several compatible options were tried and the program parameter values (e.g., move limits and convergence criteria on the absolute and relative changes in objective function between two successive iterations) were adjusted until the closed form and numerical solution agreed within as few iterations as possible. As a result of these numerical experiments, the popular BFGS variable metric method for unconstrained minimization emerged as the one of choice for use in the combined control-structure optimization examples that follow. During the one dimensional line search, the minimum is located by first computing the bounds, then using polynomial interpolation.

Example 1. The cantilever beam of Fig. 1 resembling a flexible appendage of a large structure is modelled by three finite elements with two degrees-of-freedom (dof) at each node. The structural design variables $\alpha_1, \alpha_2, \alpha_3$ determine the cross sectional areas $\tilde{\alpha}_1, \tilde{\alpha}_2, \tilde{\alpha}_3$ of the elements by the relation $\tilde{\alpha}_i = \alpha_i^2 + \tilde{\alpha}_0$. The disturbance $\boldsymbol{v}$ represents a transverse sound pressure modelled by uncorrelated unit impulses at $t = 0$ concentrated at the three nodal transverse dof. Thus $\mathbf{Q}_v$ = identity. The control force $\boldsymbol{u}$ is applied at the free end along the transverse dof direction. With the J_s given by (3.4), we seek the minimum of (5.4a) for $\lambda \in [0, 1]$, subject to conditions (3.13). Here, the

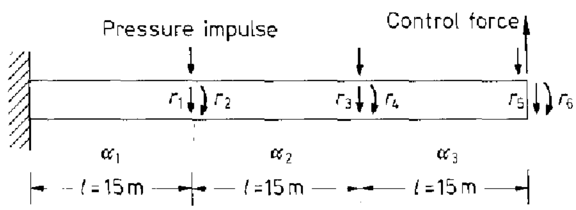

1

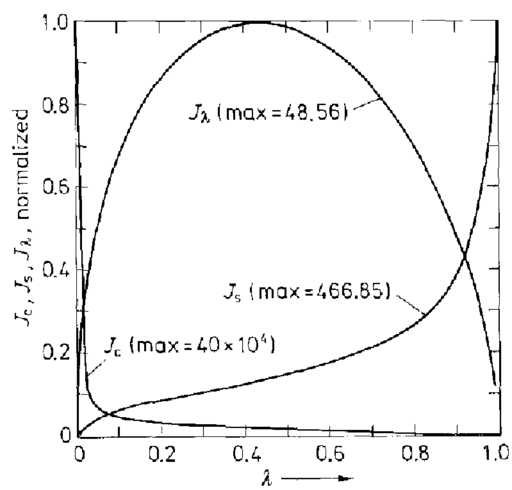

2

Figs. 1 and 2. 1 Example 1. Cantilever beam problem: mass density = 1660 Kg/m^3, modulus = 9.56×10^{10} N/m^2, modal damping = 0.5%; disturbance = transverse pressure impulse concentrated at the nodes, response energy weighted by $\mathbf{D}_o$ = Diag(**K**, **M**) $\times 10^2$, control energy weighted by $\mathbf{R} = 1 \times 10^{-4}$; design variables: $\alpha_1, \alpha_2, \alpha_3 \geq 1 \times 10^{-7}$. **2** Cantilever beam optimization weighting matrices were taken as $\mathbf{D}_o = 10^2 \times \text{diag}(\mathbf{K}, \mathbf{M})$, and $\mathbf{R} = 10^{-4}$. Additionally, $\nu = -15.75$ and $\alpha_0 = 10^{-7}$.

Table 1 lists the family of optimal designs that minimize J_λ, $\lambda \in [0, 0.99]$ along with the corresponding values for J_c, J_s and J_λ. The variations of the Pareto optimal $J_c(\lambda)$, $J_s(\lambda)$ and $J_\lambda(\lambda)$ are shown in Fig. 2. A number of observations can be made from Table 1 and Fig. 2:

Table 1. Optimal designs of Example 1

	Optimal design (m²) × 10^{-6}					
λ	$\tilde{\alpha}_1$	$\tilde{\alpha}_2$	$\tilde{\alpha}_3$	J_c	J_s	J_λ
0.000	0.2000	0.2000	0.2000	405040.8076	0.0149	0.1354 e^{-6}
1.000 e^{-6}	0.8514	1.6590	1.0774	63057.2500	0.0893	0.1035
1.000 e^{-5}	2.3723	4.9960	3.1182	21379.1719	0.2611	0.3890
1.00 e^{-4}	7.1029	15.2422	9.2979	6972.8296	0.7879	1.3299
0.005	48.5681	100.2801	64.0088	882.0427	5.3001	9.2907
0.010	68.3854	138.5623	88.9325	599.5123	7.3674	12.8250
0.020	96.9295	191.4519	124.8242	400.0817	10.2888	17.5360
0.040	136.4523	262.4428	173.9179	265.9015	14.2630	23.6820
0.100	216.3664	405.5988	274.5324	148.6908	22.3228	34.1500
0.200	315.0205	573.3193	393.8050	91.9583	31.9254	42.9630
0.300	401.4612	717.4291	496.6321	66.9654	40.2265	47.1600
0.400	487.2732	861.6987	600.1050	51.5784	48.5320	48.5550
0.500	583.8055	1023.7800	716.5723	40.2783	57.8715	47.7690
0.600	679.0599	1212.8807	852.7400	31.5295	68.7907	45.0100
0.700	841.8542	1452.9294	1025.8928	24.2444	82.6848	40.2150
0.800	1063.1860	1819.2931	1291.5679	17.4467	103.9338	32.9930
0.900	1518.2933	2564.1045	1834.4232	10.5185	147.3288	22.1140
0.940	1946.9393	3263.9368	2349.5378	7.3549	188.2543	15.8510
0.980	3375.1292	5451.4126	3998.1328	3.3907	319.3344	6.6362
0.990	5057.3018	7818.5498	5873.0239	1.9442	466.8470	2.8740

Table 2. Optimal designs for Example 1

Initial design (m²) × 10^{-6}			Optimal design (m²) × 10^{-6}					
$\tilde{\alpha}_1$	$\tilde{\alpha}_2$	$\tilde{\alpha}_3$	$\tilde{\alpha}_1$	$\tilde{\alpha}_2$	$\tilde{\alpha}_3$	J_c	J_s	J
$\lambda = 0.200$								
216.3664	405.5988	274.5324	315.0205	573.3193	393.8050	91.9583	31.9254	42.9630
702.3500	405.5988	274.5324	310.7759	572.5534	392.6549	92.5688	31.7720	42.9650
405.5988	405.5988	274.5324	314.3820	573.3193	394.2019	91.9817	31.9194	42.9630
274.5324	274.5324	405.5988	315.5886	570.4977	393.6462	92.1948	31.8653	42.9630
0.1000	0.1000	0.1000	312.4349	574.4692	393.5273	92.1295	31.8827	42.9640
$\lambda = 0.700$								
697.0599	1212.8807	852.7400	841.8542	1452.9294	1025.8928	24.2444	82.6848	40.2150
2025.1000	1212.8807	852.7400	844.6998	1460.3334	1032.0515	24.0747	83.0934	40.2150
1212.8807	1212.8807	852.7400	834.0389	1461.5564	1033.9153	24.1539	82.9048	40.2160
852.7400	852.7400	1212.8807	845.9210	1460.3334	1030.9595	24.0734	83.0966	40.2150
0.1000	0.1000	0.1000	845.2230	1459.4165	1030.9595	24.0901	83.0564	40.2150
$\lambda = 0.900$								
1063.1860	1819.2931	1291.5679	1518.2933	2564.1045	1834.4232	10.5185	147.3288	22.1140
3192.3499	1819.2931	1291.5679	1522.1923	2572.0098	1839.4806	10.4740	147.7487	22.1130
1819.2931	1819.2931	1291.5679	1524.0654	2560.6624	1835.1942	10.5107	147.4061	22.1140
1291.5679	1291.5679	1819.2931	1503.5229	2568.1567	1831.3407	10.5534	146.9852	22.1140
0.1000	0.1000	0.1000	1522.4263	2571.2998	1841.5397	10.4699	147.7881	22.1130

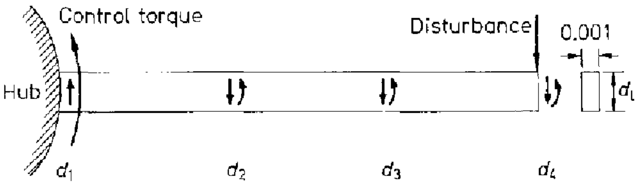

3

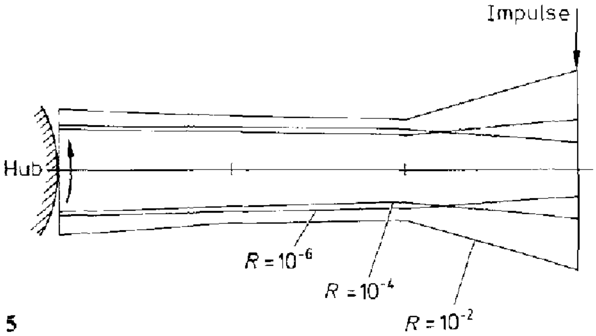

5

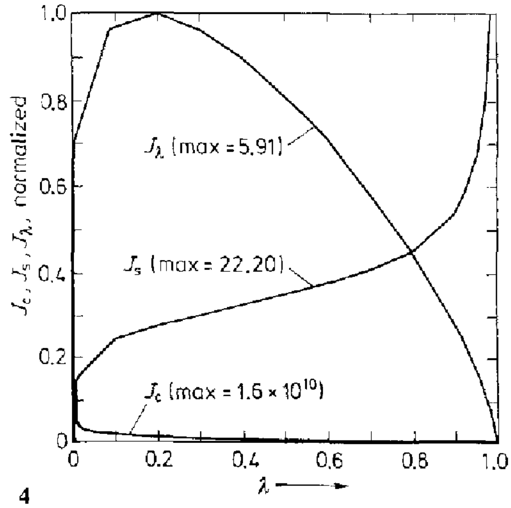

4

Figs. 3–5. 3 Example 2. Hub-beam problem; mass density = 1660 Kg/m^3, modulus = 9.56×10^{10} N/m^2; modal damping = 0.5%; disturbance = unit impulse, response energy weighted to minimize end displacement, R = 1×10^{-4}; design variables; $d_1, \ldots, d_4 \geq 0.001$. 4 Hub-beam optimization. 5 Optimum shapes

(i) The noncommensurate nature of the two costs J_c and J_s is apparent as the weight is shifted between them: while J_c is a strictly decreasing function of λ, J_s is a strictly increasing function of λ. This is consistent since a stiffer structure requires less control energy.

(ii) Except near $\lambda = 0$, the optimal structural shapes that minimize J_λ for the disturbance, choice of $\mathbf{D}_o$ and $\mathbf{R}$, and control forces described above correspond to $\tilde{\alpha}_1, \tilde{\alpha}_3 < \tilde{\alpha}_2$. This is a physically plausible optimal shape for the given distribution of disturbance and control force. The presence of the control force at the free end provides a sustaining dynamic reaction to the uniform pressure distribution along the beam. As a result, the cantilever beam (with highest strain energy at the fixed end) is made to act as a "propped" cantilever, with highest strain energy shifted away from the fixed end. Other choices of disturbance, control location and D_o, R are expected to alter the optimal beam shape.

(iii) Although the design at $\lambda = 0$ is guaranteed to be globally optimal (Proposition 4.1), it is possible that designs generated as λ is continued may be only locally optimal. To assess this possibility, the optimal designs listed for $\lambda = 0.200$, $\lambda = 0.700$ and $\lambda = 0.900$ were re-examined separately. For each case, the minimization was restarted with randomly selected initial α_i values. In most cases, the minimization converged to the same or to a higher minimum than obtained in Table 1. This is shown in Table 2.

Example 2. The beam in this example (Fig. 3) simulates a flexible appendage (length = 45 m) attached to a rigid hub (radius = 10 m and inertia = 50 Kg·m^2) to which a control torque is applied to counteract the transverse unit impulse at the free end. The beam is modelled by three finite elements of constant width = 0.001 m, but whose nodal depths $d_1, \ldots, d_4$ represent design variables having a lower bound = 0.001 m. Here again, J_s represents the total mass of the flexible beam (excluding the hub). For the control objective J_c, the response energy is weighted by $\mathbf{D}_o$ so as to minimize the transverse free end displacement, and $\mathbf{R}$ is taken = 10^{-4}.

Table 3 and Fig. 4 represent analogous results to those presented for Example 1 in Table 1 and Fig. 2. In addition to observation (i) of the previous example—which holds here as well—the following remarks can be made with reference to the results of this example:

(i) For small values of λ (e.g., $\lambda = 0.1$), where the total mass J_s dominates the minimization of J_λ, the optimal shapes tend to have a small slope from $d_1 \to d_2 \to d_3$, followed by a sharper

Table 3. Optimal designs for Example 2

	Optimum design (m)						
λ	d_1	d_2	d_3	d_4	J_c	J_s	J_λ
0.000	0.001	0.001	0.001	0.001	$1.6 \times 10^{+10}$	0.075	0.075
0.0001	0.02404	0.02363	0.02291	0.01366	3355.26	1.628	1.963
0.001	0.03552	0.03485	0.03359	0.02065	482.6	2.404	2.884
0.010	0.05223	0.05134	0.04940	0.03043	70.78	3.54	4.21
0.100	0.07699	0.07559	0.07157	0.05303	10.03	5.28	5.757
0.200	0.08759	0.08563	0.08031	0.06659	5.33	6.05	5.906
0.300	0.09550	0.09267	0.08657	0.07847	3.54	6.62	5.703
0.400	0.10258	0.09867	0.09187	0.09085	2.56	7.15	5.31
0.500	0.10944	0.10389	0.09670	0.10470	1.93	7.66	4.79
0.600	0.11715	0.10948	0.10135	0.12176	1.46	8.22	4.17
0.700	0.12657	0.11576	0.10681	0.14516	1.08	8.92	3.43
0.800	0.13944	0.12322	0.11304	0.18055	0.77	9.87	2.59
0.900	0.16369	0.13641	0.12430	0.24923	0.47	11.63	1.59
0.920	0.17299	0.14104	0.12893	0.27374	0.41	12.28	1.355
0.940	0.18542	0.14815	0.13565	0.30544	0.34	13.18	1.107
0.960	0.20578	0.16117	0.14818	0.35131	0.26	14.64	0.83
0.980	0.25035	0.19468	0.18421	0.42401	0.16	17.83	0.52
0.990	0.29401	0.25488	0.24878	0.48165	0.09	22.20	0.32

slope from $d_3 \to d_4$. As λ increases, minimizing J_s becomes less important than minimizing J_c (tip displacement response energy plus control energy). As a result, the beam becomes gradually stiffer, and the monotonic slope from $d_1 \to d_2 \to d_3 \to d_4$ associated with small λ values gradually disappears at $\lambda \simeq 0.45$, then gives way to a pronounced inflection of slope for $d_3 \to d_4$ for $\lambda > 0.45$. This results in a larger allocation of mass at the tip. This type of shape is physically consistent with the requirements of the two parts of the control objective J_c: a stiffer structure near the hub that is reduced toward the tip (free end) makes best distribution of mass, while minimizing the tip displacement response. On the other hand, a large mass at the tip (where the disturbance exists) makes the disturbance less effective—thus requiring less control effort.

(ii) To confirm the above interpretation, the case of $\lambda = 0.7$ in Table 3 (i.e. $\mathbf{R} = 10^{-4}$) was re-examined for smaller and larger values of **R**; $\mathbf{R} = 10^{-6}$ and $\mathbf{R} = 10^{-2}$, respectively. As Fig. 5 shows, smaller values of **R** give more weighting to the tip displacement response energy part of J_c, thus giving rise to the optimum shape being a stiffer structure near the hub which is reduced toward the tip. Conversely, larger values of **R** (e.g. $\mathbf{R} = 10^{-2}$) give more relative weighting to the control energy part of J_c, which is best minimized by the presence of the heavier tip mass. It is interesting to note the similar effect of varying **R** and varying λ on the optimal shapes.

(iii) Of general interest to problems in combined optimization—at least numerically—is the question as to the degree of "roughness" of the hyper-surface $J_\lambda(\alpha)$. A partial answer to this question is provided in Fig. 6 after introducing idealizations that reduce the number of variables from four $(d_1, \ldots, d_4)$ to only two (d_3, d_4), so that a three dimensional plot could be generated. Figure 6 shows such a surface in the neighborhood of the optimum for the case $\lambda = 0.7$ in Table 3. This is achieved by fixing $d_1 = 0.13$, allowing d_3 and d_4 to assume various values larger and smaller than those in Table 2 for $\lambda = 0.7$, and letting $d_2 = \frac{1}{2}(d_1 + d_3)$. Assuming that the idealizations above (which led to reducing the dimensionality of the J_λ surface) did not alter the basic topology of the J_λ surface, it appears from Fig. 6 that J_λ is a smooth function of the design variables—at least in the neighborhood of the minimum. Furthermore, with these idealizations it appears that J_λ is relatively flat near the minimum along the d_4 axis, and that the optimum shape is some linear combination of the four basic shapes depicted at the corners.

Example 3. This last example illustrates the use of the Newton method discussed in Sect. 5 to solve for optimal designs. Again we consider the three-element cantilever beam model (Fig. 1) which is discussed in Example 1. The structural design variables $\alpha_1, \alpha_2, \alpha_3$, determine the circular

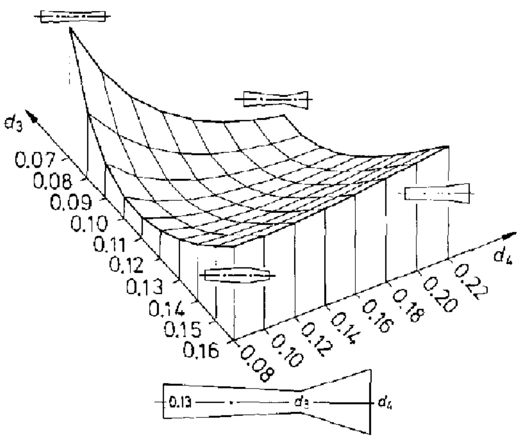

Fig. 6. $J_\lambda(d_3, d_4)$ surface near the minimum, $\lambda = 0.7$

Table 4. Optimal designs for Example 3

	Optimal design (m²) × 10^{-6}					
λ	$\tilde{\alpha}_1$	$\tilde{\alpha}_2$	$\tilde{\alpha}_3$	J_c	J_s	J_λ
0.0	0.2	0.2	0.2	5770000.	0.015	$0.135e^{-6}$
0.1	138.0	227.0	179.0	44.1	13.5	16.0
0.2	175.0	282.0	224.0	24.0	17.0	17.7
0.3	203.0	325.0	259.0	15.9	19.6	17.8
0.4	230.0	366.0	292.0	11.4	22.1	17.0
0.5	257.0	407.0	327.0	8.38	24.7	15.7
0.6	288.0	453.0	364.0	6.15	27.5	13.8
0.7	325.0	508.0	410.0	4.37	31.0	11.4
0.8	377.0	586.0	475.0	2.87	35.8	8.43
0.9	477.0	728.0	597.0	1.50	44.9	4.68

cross-sectional areas $\tilde{\alpha}_1, \tilde{\alpha}_2, \tilde{\alpha}_3$ as in Example 1. The disturbance $\boldsymbol{v}$ represents a transverse sound pressure modeled by uncorrelated unit impulses at $t = 0$ concentrated at the three nodal transverse degrees of freedom (i.e., $\mathbf{Q}_v = \mathbf{I}$, where $\mathbf{I}$ is the identity). The control force $\boldsymbol{u}$ is applied at the free end along the transverse direction. The extremal values of the functional J_λ are solved for $\lambda \in [0, 1]$ by means of an iteration of the form (5.3), where the connection with the optimization problem is given by (5.2) and the formulas given in (5.11) are used to make the necessary approximations. Here again we use $\boldsymbol{v} = -15.75$, $\boldsymbol{\alpha}_0 = 10^{-7}$, $\mathbf{V} = 0$, $\mathbf{R} = 10^{-4}$, but $\mathbf{D}_o = 10 \times \mathbf{I}$.

Table 4 lists the calculated family of optimal design $\tilde{\alpha}_i$ that minimize J_λ for $\lambda \in [0, 1]$ along with the corresponding values for J_c, J_s and J_λ. The general observations of Example 1 ((i), (ii), (iii)) also apply here.

7 Conclusions

An approach for combined control-structure optimization keyed to enhancing early design trade-offs has been outlined and illustrated by numerical examples. The approach employs a homotopic strategy and appears to be effective for generating families of designs that can be used in these early trade studies.

Analytical results were obtained for classes of structure/control objectives with LQG and LQR costs. For these, we have demonstrated that global optima can be computed for small values of the homotopy parameter. Conditions for local optima along the homotopy path were also given. Details of three numerical examples employing the LQR control cost were given showing variations of the optimal design variables along the homotopy path. The results of the second example suggest that introducing a second homotopy parameter relating the two parts of the control index in the LQG/LQR formulation might serve to enlarge the family of Pareto optima, but its effect on modifying the optimal structural shapes may be analogous to the original parameter λ.

Acknowledgements

The research described in this paper was performed as part of the Control Structure Interaction (CSI) Program at the Jet Propulsion Laboratory, California Institute of Technology, under contract with the National Aeronautics and Space Administration.

Appendix

Proof of Proposition 4.1. Let $\mathbf{Z}^*$ and $\mathbf{P}^*$ denote the unique zeros of (3.13b) and (3.13c) corresponding to $\boldsymbol{\alpha}^*$, and note that if $x^* = (\boldsymbol{\alpha}^*, \mathbf{Z}^*, \mathbf{P}^*)$ then for $(\boldsymbol{h}, \mathrm{S}, \mathrm{T}) \in R^{na} \times \boldsymbol{\Sigma} \times \boldsymbol{\Sigma}$

$$\frac{\partial \mathrm{H}(0, x^*)}{\partial x} : (\boldsymbol{h}, \mathrm{S}, \mathrm{T}) \rightarrow \begin{pmatrix} \nabla_\alpha^2 J_s(\boldsymbol{h}) \\ \mathbf{A}_c\mathbf{S} + \mathbf{S}\mathbf{A}_c^T + \nabla_\alpha \mathbf{A}_c(\boldsymbol{h})\mathbf{Z} + \mathbf{Z}\nabla_\alpha \mathbf{A}_c^T(\boldsymbol{h}) - \mathbf{B}_1\mathbf{R}^{-1}\mathbf{B}_1^T\mathbf{T}\mathbf{Z}_* - \mathbf{Z}_*\mathbf{T}\mathbf{B}_1\mathbf{R}^{-1}\mathbf{B}_1^T + \nabla_\alpha[\mathbf{B}_2\mathbf{Q}_v\mathbf{B}_2^T + \mathbf{V}](\boldsymbol{h}) \\ \mathbf{A}_c^T\mathbf{T} + \mathbf{T}\mathbf{A}_c + \nabla_\alpha \mathbf{A}^T(\boldsymbol{h})\mathbf{P}^* + \mathbf{P}^*\nabla_\alpha \mathbf{A}_c(\boldsymbol{h}) + \nabla_\alpha \mathbf{D}_o(\boldsymbol{h}) - \nabla_\alpha[\mathbf{B}_1\mathbf{R}^{-1}\mathbf{B}_1^T](\boldsymbol{h})\mathbf{P}^* \end{pmatrix}.$$

It follows from the second order sufficiency condition that $\nabla_\alpha^2 J_s(\boldsymbol{h})$ vanishes if and only if $\boldsymbol{h} = 0$. Since $\mathbf{A}_c$ is stable, if $\boldsymbol{h} = 0$, the third term on the right above vanishes if and only if $\mathbf{T} = 0$. Furthermore, given that both $\boldsymbol{h}$ and $\mathbf{T}$ are zero, the second term on the right above vanishes if and only if $\mathbf{S} = 0$. Hence, the null space of $\partial\mathbf{H}/\partial\mathbf{x}$ consists of the zero vector and thus $\partial\mathrm{H}/\partial\mathbf{x}$ is invertible at $(0, x^*)$. The implicit function theorem then implies that we can uniquely solve $\mathrm{H}(\lambda, x(\lambda)) = 0$ in a neighborhood about $\lambda = 0$ with $\lambda \rightarrow x(\lambda)$ smooth.

Now choose a closed ball $\mathbf{B}$ containing $(0, x^*)$ so large that all global optima for J_λ are contained in $\mathbf{B}$ for $\lambda \in [0, 1/2]$. Such a $\mathbf{B}$ exists by the coercivity of J_s. Suppose there exists a sequence $\{(\lambda_n, x_n')\} \subset \mathbf{B}$ with $\lambda_n \rightarrow 0$ such that $\mathbf{H}(\lambda_n, x_n') = 0$ and $x_n' \neq x(\lambda_n)$ for all n. (If no such sequence exists, then for λ sufficiently small the only solutions to $\mathbf{H}(\lambda, x) = 0$ with $(\lambda, x) = 0$ with $(\lambda, x) \in \mathbf{B}$ are of the form $(\lambda, x(\lambda))$, and we would be done since $\mathbf{B}$ contains all global optimal solutions for $\lambda \in [0, 1/2]$.) Since $\mathbf{B}$ is compact there exists a subsequence x_{nk} that has a limit point x_0 in $\mathbf{B}$.

Suppose first that $x_0 = x^*$, and recall that the implicit function theorem implies that solutions to $\mathbf{H}(\lambda, x) = 0$ in a neighborhood of $(0, x^*)$ are unique. Thus it follows that for $\mathbf{k}$ sufficiently large, $x_{nk}' = x(\lambda_{nk})$; and consequently x_{nk} is not distinct from $x(\lambda_{nk})$ as assumed. Therefore, $x_0 \neq x^*$. So next we claim that the subsequence $\{x_{nk}'\}$ does not contain a further subsequence consisting of global optima. For if it did, the continuity of J (as a function of λ and $\boldsymbol{\alpha}$) would imply that $J_s(\boldsymbol{\alpha}_0) \leqslant J_s(\boldsymbol{\alpha}^*)$ (where $x_0 = (\boldsymbol{\alpha}_0, \mathbf{Z}_0, \mathbf{P}_0)$), thereby contradicting the uniqueness of $\boldsymbol{\alpha}^*$. Now since the global optima exist (and in fact are contained in $\mathbf{B}$ for $\lambda \in [0, 1/2]$), it follows that for λ sufficiently small these optima are precisely those obtained from the unique solutions to $\mathbf{H}(\lambda, x) = 0$ in a neighborhood of $(0, x^*)$. □

Proof of Lemma 4.3. We first argue that for almost every $\nu \in R^{na}$, zero is a regular value of $\mathbf{H}$. To establish this define $\mathbf{Y}: R^{na} \rightarrow \boldsymbol{\Sigma}_+ \times \boldsymbol{\Sigma}_+$ as in the proof of Proposition 4.2. Sard's theorem implies that for almost every $\nu \in R^{na}$, zero is a regular value of $\mathbf{H}_1(\lambda, \boldsymbol{\alpha}, \mathbf{Y}(\boldsymbol{\alpha}))$. Hence, for almost every $\boldsymbol{\nu}$,

$$\dim \mathbf{N}\left(\left[\frac{\partial \mathbf{H}_1}{\partial \lambda} \quad \frac{\partial \mathbf{H}_1}{\partial \mathbf{x}}\begin{pmatrix} \mathbf{I} \\ \mathbf{Y}_* \end{pmatrix}\right]\right) = 1,$$

where $\mathbf{Y}_*$ again denotes the differential of $\mathbf{Y}$. To prove that zero is regular when this condition holds it is sufficient to show that $\dim \mathbf{N}(\mathbf{H}_*) = 1$ at every zero of $\mathbf{H}(\lambda, \boldsymbol{\alpha}, \mathbf{Z}, \mathbf{P})$.

So assume that $[r\boldsymbol{h}\mathbf{S}\mathbf{T}] \in \mathbf{N}(\mathbf{H}_*)$. Noting that $\mathbf{H}_2$ and $\mathbf{H}_3$ are independent of λ, it follows that

$$\frac{\partial \mathbf{H}_2}{\partial \boldsymbol{x}}\begin{bmatrix} \boldsymbol{h} \\ \mathbf{S} \\ \mathbf{T} \end{bmatrix} = \frac{\partial \mathbf{H}_3}{\partial \boldsymbol{x}}\begin{bmatrix} \boldsymbol{h} \\ \mathbf{S} \\ \mathbf{T} \end{bmatrix} = 0.$$

But this implies that

$$\begin{bmatrix} \mathbf{S} \\ \mathbf{T} \end{bmatrix} = \mathbf{Y}_*(\boldsymbol{\alpha})\boldsymbol{h}.$$

Hence,

$$\dim \mathbf{N}(\mathbf{H}_*) = \dim \left\{ \begin{bmatrix} r \\ \boldsymbol{h} \end{bmatrix} : \frac{\partial \mathbf{H}_1}{\partial \lambda} r + \frac{\partial \mathbf{H}_1}{\partial \boldsymbol{x}} \begin{bmatrix} \mathbf{I} \\ \mathbf{Y}_* \end{bmatrix} \boldsymbol{h} = 0 \right\} = 1.$$

And indeed zero is a regular value of $\mathbf{H}$ for almost every $\boldsymbol{v} \in R^{na}$.

As discussed above the component of $\mathbf{H}^{-1}(0)$ containing $(0, \boldsymbol{x}^*)$ is diffeomorphic to a circle or $\mathbf{R}$. Recalling the argument in Proposition 4.1, the solution path cannot return to $(0, \boldsymbol{x}^*)$ because of the uniqueness of the solution in a neighborhood containing $(0, \boldsymbol{x}^*)$. Hence, the result follows. □

Proof of Theorem 4.4. Lemma 4.3 implies that for almost every $\boldsymbol{v}$ we may assume that zero is a regular value of $\mathbf{H}$. We will assume that such a choice has been made, and denote the component containing $(0, \boldsymbol{x}^*)$ as C. Standard topological arguments using the regularity of $\mathbf{C}$, the uniqueness of the solution at $\lambda = 0$, and the fact that $\partial \mathbf{H}/\partial \boldsymbol{x}$ is invertible at $(0, \boldsymbol{x}^*)$ (cf. Proposition 4.1), show that the path can be continued in λ so long as it remains bounded.

Now assume that $\det(\partial \mathbf{H}/\partial \boldsymbol{x}) = 0$ at only a finite number of points of C. (This will be proven later.) There are two cases to consider under this assumption:

(i) λ is ultimately increasing along C, or
(ii) λ is ultimately decreasing along C.

Let $(\lambda, \boldsymbol{\alpha}(\lambda), \mathbf{Z}(\boldsymbol{\alpha}(\lambda)), \mathbf{P}(\boldsymbol{\alpha}(\lambda)))$ be a parameterization of C, and let $\mathbf{M}(\boldsymbol{\alpha}) = \mathbf{B}_2(\boldsymbol{\alpha})\mathbf{Q}_v\mathbf{B}_2^T(\boldsymbol{\alpha}) + \mathbf{V}$. Then observe that if λ is either strictly increasing or decreasing

$$\begin{aligned} \frac{d}{d\lambda} J_\lambda(\boldsymbol{\alpha}(\lambda)) &= \frac{d}{d\lambda}\{(1-\lambda)J_s(\boldsymbol{\alpha}(\lambda)) + \langle \boldsymbol{v}, \boldsymbol{\alpha}(\lambda) \rangle + \lambda \operatorname{tr}[\mathbf{P}(\boldsymbol{\alpha}(\lambda))\mathbf{M}(\boldsymbol{\alpha}(\lambda))]\} \\ &= -J_s(\boldsymbol{\alpha}(\lambda)) + \operatorname{tr}\{\mathbf{P}(\boldsymbol{\alpha}(\lambda))\mathbf{M}(\boldsymbol{\alpha}(\lambda))\} + \sum_{i=1}^{n_a} -\frac{\partial J_\lambda}{\partial \alpha_i}\frac{\partial \alpha_i}{\partial \lambda} \\ &= -J_s(\boldsymbol{\alpha}(\lambda)) + \operatorname{tr}\{\mathbf{P}(\boldsymbol{\alpha}(\lambda))\mathbf{M}(\boldsymbol{\alpha}(\lambda))\}, \end{aligned}$$

since $\nabla_{\alpha} J$ vanishes along C.

We now consider Case (i) where λ is ultimately increasing. Define $J^-(\lambda) = J_\lambda(\boldsymbol{\alpha}(\lambda))/\lambda$, and compute its derivative to obtain

$$\begin{aligned} \frac{d}{d\lambda} J^-(\lambda) &= \frac{1}{\lambda}\frac{d}{d\lambda}\{J_\lambda(\boldsymbol{\alpha}(\lambda))\} - \frac{1}{\lambda^2} J_\lambda(\boldsymbol{\alpha}(\lambda)) \\ &= -\frac{1}{\lambda}[-J_s(\boldsymbol{\alpha}(\lambda)) + \operatorname{tr}\{\mathbf{P}(\boldsymbol{\alpha}(\lambda))\mathbf{M}(\boldsymbol{\alpha})\}] - \frac{1}{\lambda^2} J_\lambda(\boldsymbol{\alpha}(\lambda)) \\ &= -\frac{1}{\lambda^2}[J_s(\boldsymbol{\alpha}) - \langle \boldsymbol{v}, \boldsymbol{\alpha}(\lambda) \rangle]. \end{aligned}$$

The coercivity assumption on J_s implies then that $J^-(\lambda)$ is a decreasing function for $|\boldsymbol{\alpha}|$ sufficiently large. Therefore $|\boldsymbol{\alpha}(\lambda)|$ must remain bounded as λ increases. (For if not, $J_\lambda(\boldsymbol{\alpha}(\lambda))$ would grow unboundedly, and hence, so would J^-.) Now Assumption A together with the continuity of the maps $\boldsymbol{\alpha} \to \mathbf{P}(\boldsymbol{\alpha}), \mathbf{Z}(\boldsymbol{\alpha})$ in turn imply that $\mathbf{P}(\boldsymbol{\alpha}(\lambda))$ and $\mathbf{Z}(\boldsymbol{\alpha}(\lambda))$ (the zeros of (3.13c) and (3.13b), respectively), also remain bounded. Thus if λ is ultimately increasing, $|\boldsymbol{x}(\lambda)|$ remains bounded.

Next we consider the case in which λ is ultimately decreasing. The argument is essentially the same except we use the function $J^+(\lambda) = 1/(1-\lambda)J_\lambda(\boldsymbol{\alpha}(\lambda)) - 1/(1-\lambda)\langle \boldsymbol{v}, \boldsymbol{\alpha}(\lambda)\rangle$. Differentiating this function we obtain

$$d/d\lambda J^+(\lambda) = \frac{1}{(1-\lambda)^2} \operatorname{tr}[\mathbf{P}(\boldsymbol{\alpha}(\lambda))\mathbf{M}(\boldsymbol{\alpha}(\lambda))] > 0.$$

Thus we see that J^+ is an increasing function of λ, and hence must decrease with decreasing λ. Then for the same reasons as above we find that $|\boldsymbol{x}(\lambda)|$ must remain bounded as λ decreases.

It remains to show that $\det(\partial \mathbf{H}/\partial \boldsymbol{x})$ indeed vanishes at only a finite number of points along C. To begin, we define the variety $\mathbf{V}$

$$\mathbf{V} = \{(\lambda, \boldsymbol{x}) \in C \times C^{n_a + n_x(n_x+1)}: \mathbf{H}(\lambda, \boldsymbol{x}) = 0\},$$

where C denotes the complex plane. Here we are interpreting $\mathbf{H}$ in the sense of a polynomial system of equations in the indeterminants α_i, z_{ij}, and p_{ij}, where the z_{ij} and p_{ij} are the entries of the matrices $\mathbf{Z}$ and $\mathbf{P}$ respectively in (3.13b)–(3.13c). Furthermore, we are considering all complex solutions to this system of equations. Hence the component C is a subset of $\mathbf{V}$.

We will show that C is contained in a single irreducible subvariety of $\mathbf{V}$. To see this first note that since zero is a regular value of $\mathbf{H}$, the matrix $\mathbf{H}_*$,

$$\mathbf{H}_* = [\partial \mathbf{H}/\partial \lambda \quad \partial \mathbf{H}/\partial \boldsymbol{x}]$$

has full rank at every point of C. Since all of the entries of $\mathbf{H}_*$ are real along C, $\mathbf{H}_*$ also has full rank when considered as a matrix acting on a complex vector space. Since C is connected (Lemma 4.3), and varieties are closed sets, it follows that if C is not contained in a single irreducible variety, then there must be a point, say $p \in \mathbf{C}$, with $p \in \mathbf{V}_1 \cap \mathbf{V}_2$, where $\mathbf{V}_1$ and $\mathbf{V}_2$ are irreducible subvarieties of $\mathbf{V}$ such that neither is contained in the other. Thus it follows that $\dim \mathbf{V}_1 = \dim \mathbf{V}_2 = 1$, for if one of them had dimension equal to zero, being irreducible, it would necessarily consists of the single point p, and thus be contained in the other.

Now since $\mathbf{H}_*$ has full rank, the implicit function theorem implies that in a neighborhood of p, $\mathbf{V}$ can locally be described as the graph of an analytic function of one variable. Then without loss of generality we may assume that there exists an open set $\mathbf{U}$ in $C^{n_a + n_x(n_x+1)}$ containing p and an analytic function $\boldsymbol{h}: \mathbf{W} \to \mathbf{U}$ where $\mathbf{W}$ is an open neighborhood of $0 \in C$ such that

$$\mathbf{V} \cap \mathbf{U} = \{(w, \boldsymbol{h}(w)): w \in \mathbf{W}\}.$$

But now note that if a polynomial g vanishes on $\mathbf{V}_1 \cap \mathbf{U}$ it necessarily vanishes on $\mathbf{V}_2 \cap \mathbf{U}$ as well since $g(w, \boldsymbol{h}(w))$ is an analytic function on $\mathbf{W}$ whose zero set contains limit points in $\mathbf{W}$; and thus must identically vanish on $\mathbf{W}$. The polyonomials that vanish on $V_i \cap U$ are precisely those that vanish on $\mathbf{V}_i$. Therefore $J(\mathbf{V}_1) = J(\mathbf{V}_2)$, and as $\mathbf{V}_1$ and $\mathbf{V}_2$ are both varieties, it follows that $\mathbf{V}_1 = \mathbf{V}_2$, contradicting the assumption that they are distinct. Therefore C is contained in a single irreducible variety, say $\mathbf{V}_1$.

Next consider the subvariety $\mathbf{V}_1' \subset \mathbf{V}_1$,

$$\mathbf{V}_1' = \{\lambda, \boldsymbol{x}) \in \mathbf{V}_1 : \det(\partial \mathbf{H}/\partial \boldsymbol{x}) = 0\}.$$

$\mathbf{V}_1'$ is a proper subvariety of $\mathbf{V}_1$ since we have shown in Proposition 4.1 that $\partial \mathbf{H}/\partial \boldsymbol{x}$ is invertible at $(0, \boldsymbol{x}^*)$. Thus $\dim \mathbf{V}_1' = 0$. Consequently $\mathbf{V}_1'$ consists of a finite number of points, completing the proof of the theorem. □

References

Bodder, D. S.; Junkins, L. (1984): Eigenvalue optimization algorithms for structural/control design Iterations. Amer. Contr. Conf., San Diego, CA

Fletcher, R. (1987): Practical methods of optimization. 2nd. ed., New York: Wiley

Hale, A. L.; Liskowski, K. J.; Dahl, W. E. (1985): Optimal simultaneous structural and control design of maneuvering spacecraft. AIAA, J. Guidance, 8, 86–93

Keller, H. B. (1987): Lectures on numerical methods in bifurcation problems. Berlin, Heidelberg, New York: Springer

Khot, N. S.; Eastep, F. E.; Venkayya, V. B. (1985): Simultaneous optimal structural/control modifications to enhance the vibration control of a large flexible structure. Proc. of the AIAA Guid., Nav. and Contr. Conf. 459–466

Kwakernaak, H.; Sivan, R. (1972): Linear optimal control system. New York: Wiley

Lim, K.; Junkins, J. (1989): Robust optimization of structural and controller parameters. J. Guidance, 12, 89–96

Lin, J. G. (1976): Maximal vectors and multi-objective optimization. J. Opt. Theory Appl. 18, 41–65

Milman, M.; Scheid, R.; Salama, M.; Bruno, R. (1989): Methods for combined contol-structure optimization. Proceedings of the VPI Symposium on the Dynamics and Control of Large Structures, Blacksburg, VA

Milman, M.; Salama, M.; Scheid, R.; Bruno, R.; Gibson S. (1990): Integrated control-structure design: A multiobjective approach JPL Inter. Rpt. D-6767

Morrison S. K.; Ye, Y.; Gregory, Jr., C. F.; Kosut, R.; Regelbrugge, M. E. (1988): Integrated structural/controller optimization for large space structures. AIAA Guid. and Contr. Conf., Minneapolis, MN

Salama, M.; Garba, J.; Udwadia, F. (1988): Simultaneous optimizaton of controlled structures. J. Comput. Mech. 3, 275–282

Vanderplaats, G. (1984): ADS—A fortran program for automated design synthesis. NASA CR-172460

Watson, L. T. (1986): Numerical linear algebra aspects of globally convergent homotopy methods. SIAM Rev. 26 4, 529–545

Communicated by S. N. Atluri, June 7, 1990